ROYAL NORWEGIAN COUNCIL FOR SCIENTIFIC AND INDUSTRIAL RESEARCH

PROCEEDINGS FROM THE
SEMINAR ON

SEISMOLOGY AND SEISMIC ARRAYS

OSLO, 22–25 NOVEMBER 1971

Editors: E S Husebye and H Bungum

Arranged in connection with the opening of The Norwegian Seismic Array (NORSAR) 1972

EXTRACTION OF P WAVE SPECTRA USING THE NORSAR ARRAY

I. NOPONEN

Institute of Seismology, University of Helsinki
Helsinki, Finland

E.S. HUSEBYE AND D. RIEBER-MOHN

NTNF/NORSAR
Kjeller, Norway

ABSTRACT

Using the Fast Fourier Transform as a basic tool, power spectra of short period P wave signals from 16 well recorded earthquakes and underground explosions in Central Asia and in western North America were computed. The initial data preparation included a proper line-up of incoming signals and tapering the ends of the 6.4 sec transform windows used. The spectra were smoothed and the effect of the noise carefully removed. The computed spectra are the mean power of all 132 sensors in the NORSAR array (spectraform) and the power on the array beam. The ratio of the above two spectra (beam loss) increases sharply at frequencies above 1.5 Hz being in average 12 dB at 3 cps. Earthquakes and explosions were observed to have, in average, different shapes of spectrum. The observed spectraform spectra peaked between 1 and 2 cps. The signal-to-noise ratio for the events in Central Asia peaked around 2 cps, but was more flat for events in North America due to shift of energy towards lower frequencies. At frequencies above the spectral peak spectraforming gave the most stable estimates, though a combined processing method, the average spectrum of subarray beams, also had high stability.

INTRODUCTION

In principle, frequency domain analysis of teleseismic P-wave records of underground nuclear explosions and earthquakes should manifest typical characteristics of the above source types, and thus serve as a useful diagnostic aid in classifying seismic events. Several studies of this kind have been undertaken, and

We should here like to refer to Kelly (1968), Weichert (1969), Anglin (1972), Hasegawa (1972), etc. Although the m_b:M_S discriminant has proved to be superior to any other classification criteria, a spectral discriminant is attractive due to good P-wave detectability in the m_b magnitude range 3.8-4.5.

When actually designing a spectral discriminant, we are faced with a number of problems, ranging from the stability of the spectral estimate itself to optimizing the potential differences between earthquakes and explosions. Moreover, working with data from a large aperture array, a further complicating factor is that the P-signals are only partially coherent across the array.

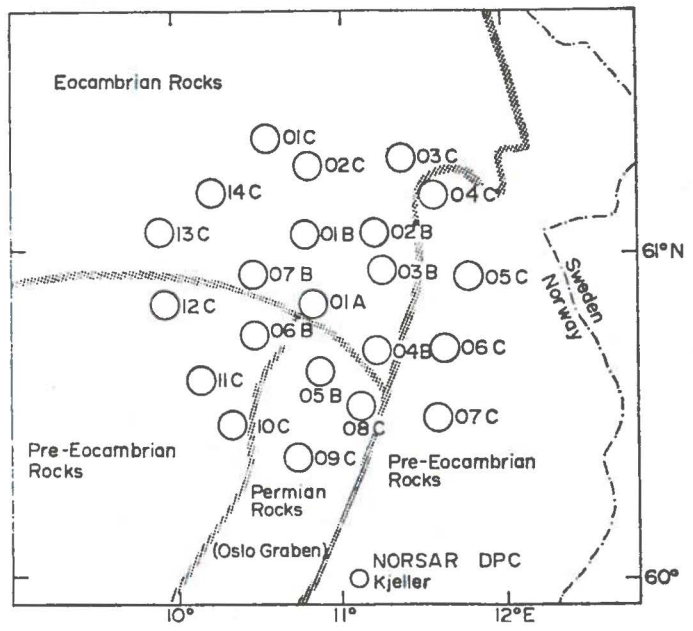

Fig 1. NORSAR array configuration with outline of geology. Each subarray is equipped with 6 vertical, short-period sensors and one 3-component long-period seismometer.

In this study different methods are compared for extracting spectral information from signals recorded at the large aperture seismic array NORSAR in Norway (see Fig 1). We have also examined the shapes of the power spectra of P-waves from different areas and source types, and investigated the frequency range where the signal-to-noise ratio of short period P-waves is highest. We will present results from spectral analysis of 15 events, earthquakes and underground explosions, in Central Asia, and of 1 underground explosion in western North America (for details see Table 1).

METHOD

To estimate the power spectrum of P-waves using a seismic array, Lacoss and Kuster (1970) considered averaging the power spectra computed for the individual seismometer outputs, the so-called spectra-form, as compared to the power spectrum for the wave form averaged over the individual seismometer outputs with suitable delays, i.e., the array or subarray beam. The reason for considering different

intricacy of the above problem, we shall base our conclusions mainly on relative rather than absolute dT/dΔ values. (For a more detailed discussion, see Doornbos and Husebye, 1972.)

Altogether, we analyzed 20 earthquakes, which are listed in Table 1, in the distance range 135-149 deg. The main results obtained are summarized in Fig 2-5, while further details are given in another paper by the authors (Doornbos and Husebye, 1972).

INTERPRETATION AND DISCUSSION

The discrepancies between current core models are mainly due to the interpretation of the precursors to the PKIKP phase as pointed out previously. An interpretation of these precursors, in particular if made in terms of branches, may have observational consequences on standard PKP waves, as well as other core phases like SKP. In turn, this may be used as an additional check on a proposed core velocity model.

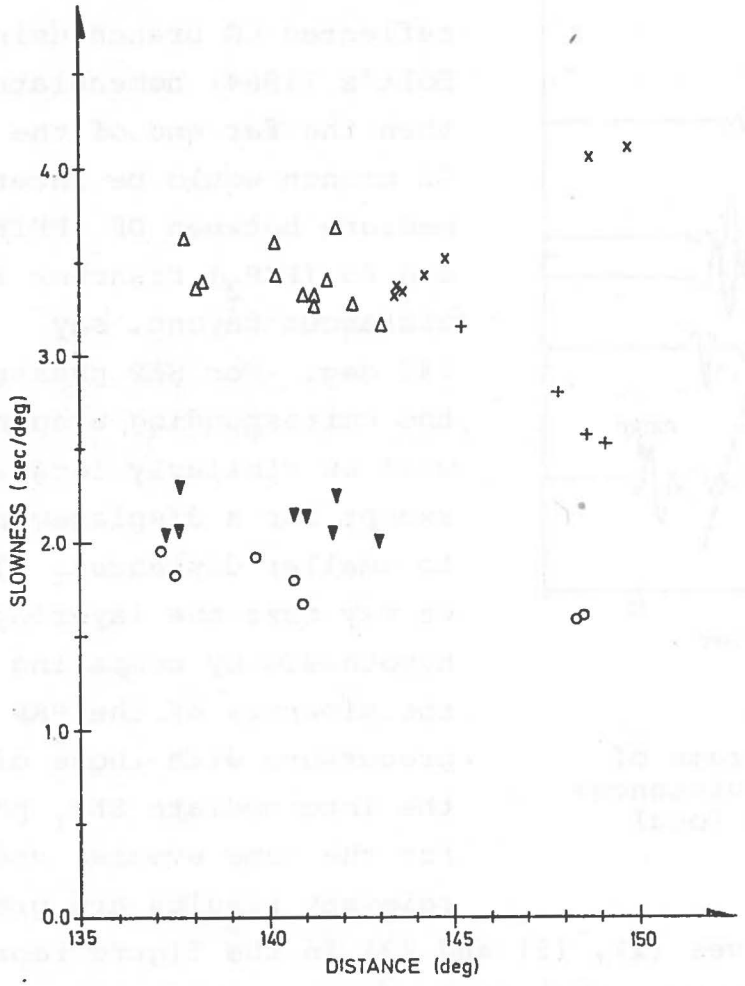

Fig 2. Corrected slownesses of PKP phases. The distances adjusted to a focal depth of 33 km. Phase identifiers: o - PKIKP, ▼ - PKiKP, Δ - precursors, + - PKP1, × - PKP2.

In Fig 2 we have displayed the results of the dT/dΔ measurements for various types of PKP phases. It is noteworthy that the Vespa process gives evidence of relatively strong reflections, PKiKP phases, from the inner core boundary. However, the most interesting feature is that the slownesses of the precursors, although somewhat scattered, have an average value about the same as for the phases near Δ~144 deg. This may

indicate that the precursor waves originate from the same region where the seismic rays forming the PKP caustic have their turning points. It thus suggests that the precursors represent diffracted waves which is consistent with the observed increase in the energy ratio between these waves and PKIKP phases with increasing distances (see Fig 3 and also Fig 4). Other precursor hypotheses in terms of reflections and/or refractions at a discontinuity in the outer core cannot be ruled out by these considerations only.

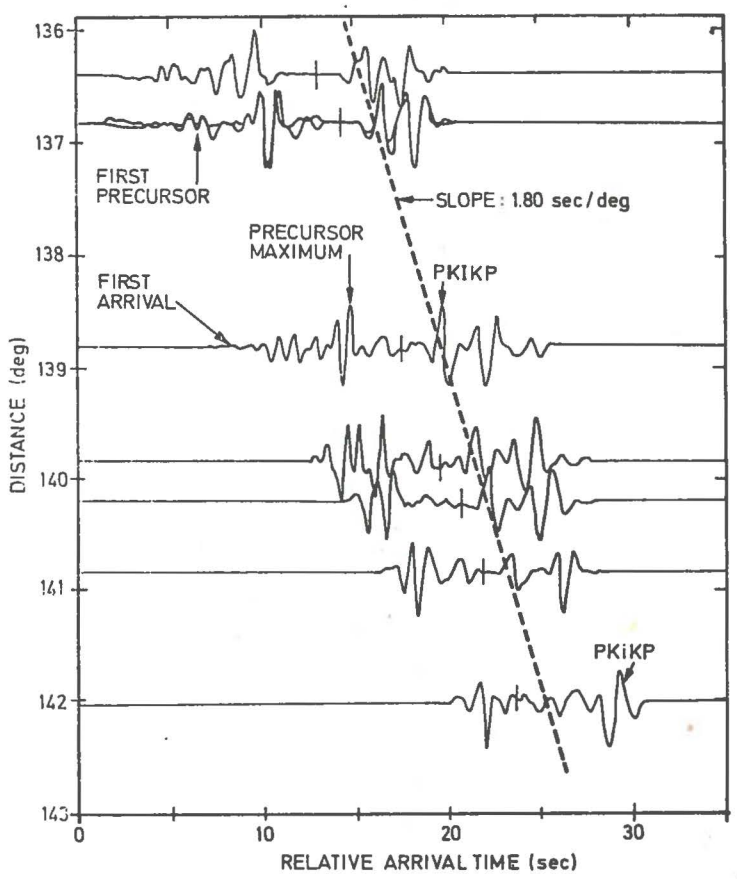

Fig 3. Composite seismograms of PKP phases. The distances are adjusted to a focal depth of 570 km.

Further constraints on current core models may be provided by taking SKP phases into account. If the precursor waves represent a refracted GH or a reflected CG branch using Bolt's (1964) nomenclature, then the far end of the GH branch would be intermediate between DF (PKIKP) and AB (PKP_2) branches at distances beyond, say 145 deg. For SKP phases, the corresponding branch will be similarly located except for a displacement to smaller distances. Thus, we may test the layering hypothesis by comparing the slowness of the PKP precursors with those of the intermediate SKP_1 phases for the same events, and relevant results are presented in Fig 5. The curves (1), (2) and (3) in the figure represent differences predicted from the model of Bolt and its revisions, A and B respectively as given by Engdahl (1968). Similar curves, namely, (4a) and (4b) for the revised Adams-Randall model (Engdahl 1968) are also included. The immediate objections against the latter model arise since it requires two different PKP precursors and two 'intermediate' SKP branches. The curve (5) is based on the revised Jeffreys' model (Engdahl 1968), if the precursors

(a) Earthquakes in Central Asia

Date	Or. Time	Lat	Long	m_b	Depth
71.06.15	07 39 37.1	41.5N	74.9E	5.6	normal
71.06.15	22 04 13.4	41.5N	79.3E	5.6	normal
71.06.16	00 58.37.4	41.5N	79.4E	5.4	normal
71.06.19	17 23 02.7	41.5N	79.3E	5.2	normal
71.07.24	11 43 38.8	39.5N	73.2E	5.6	normal
71.07.26	01 48 33.9	39.9N	77.2E	6.0	normal
71.10.28	13 30 57.1	41.9N	72.4E	5.5	22 km
72.01.02	10 27 34.9	41.8N	84.5E	5.2	normal
72.01.15	20 21 50.1	40.3N	79.0E	5.4	normal

(b) Underground Explosions in Central Asia

71.06.06	04 02 57.1	50.0N	77.8E	5.5
71.06.30	03 56 57.2	50.0N	79.1E	5.4
71.10.21	06 02 57.3	50.0N	77.6E	5.6
71.12.30	06 20 57.7	50.0N	78.9E	5.8
72.03.10	04-56 57.4	49.8N	78.2E	5.5
72.03.28	04 21 57.3	29.7N	78.2E	5.2

(c) Underground Explosion in western North America

71.07.08	14 00 00.0	37.1N	116.1W	5.5

TABLE 1

Epicentral Data (from NOAA) on Analyzed Events.

types of spectral estimates is the known variation in P-signal waveforms across a large aperture array, even in the absence of measurable noise. In other words, during beamforming we have a noise suppression proportional to the square root of the number of sensors used, but at the same time a signal loss which increases with frequency as the P-waves are only partially coherent across the array.

Following Lacoss and Kuster (1970) let the Fourier transform of the incoming signal be S(f) at some reference plane under the array and assume that the waveform variation between the sensors is caused by lateral structural variations between that plane and the surface. Then the Fourier transform of the signal at K'th sensor of the array in the absence of noise can be written as

$$S_k(f) = S(f)T_k(f) \tag{1}$$

where $T_k(f)$ represents the earth response encountered by the wave propagating to the k'th sensor. T_k consists of a part common to all sensors, let it be called T, and of perturbations specific to each sensor. Thus

$$S_k(f) = S(f)T(f)(1+H_k(f)) \tag{2}$$

where H_k represents perturbations. The H_k are considered to be random variables with zero expected value and variance σ^2. The expected value of the square of H_k is then

$$E(|H_k(f)|^2) = \sigma^2(f) \tag{3}$$

The power spectrum of a beam of K sensors is the square of the sum of the Fourier transforms of the individual seismometer outputs with suitable delays, or

$$B = \left|\frac{1}{K}\sum_{k=1}^{K} S_k\right|^2 \tag{4}$$

The expected value of B is

$$E(B) = |ST|^2\left(1+\frac{\sigma^2}{K}\right) \tag{5}$$

The average power spectrum of a group of K sensors is defined as

$$P = \frac{1}{K} \sum_{k=1}^{K} |S_k|^2 \qquad (6)$$

with expected value

$$E(P) = |ST|^2(1+\sigma^2) \qquad (7)$$

This method of computing power spectrum is called spectraforming by Lacoss and Kuster. The average power from sensors is larger than the power of beam by a factor of

$$\frac{E(P)}{E(B)} = \frac{1+\sigma^2}{1+\frac{\sigma^2}{K}} \qquad (8)$$

Beam loss increases with increasing variance σ^2, i.e., with increasing signal dissimilarity.

If the analyzed record contains in addition to signal also noise, we first estimate the noise power spectrum by analyzing record sections prior to the signal onset. By subtracting the noise power from the original spectrum containing both signal and noise power, we get a more correct estimate of the signal power spectrum. When subtracting noise estimate from spectrum obtained by beamforming, we have used the average noise power spectrum of single sensors divided by the number of sensors used, thus simulating the expected reduction of random noise due to beamforming. In addition to the arguments presented by Lacoss and Kuster, it has to be noted that when subtracting the "noise" record from the signal power spectrum, the results can evidently be of either sign or zero in some frequency bands even if no signal power is present. In such cases it was decided that signal energy is present only when the signal plus noise-to-noise ratio was as large as to give a 99% confidence of making the right decision. The actual ratio required depended on the processing method, the number of sensors and number of record blocks used in estimating the noise.

The signal length or duration used in our spectral analysis was 6.4 sec for all events. However, the beamforming losses and S/N ratios measured may depend on the sample length used, especially on the array beam level. In general, signal correlation decreases with the distance from signal onset and increasing signal length (Bungum and Husebye, 1971). On the subarray beam level we failed to observe larger signal beam losses when the sample length was increased to 10 sec. Anyway, the signal duration of 6.4 sec used in analysis was a compromise between a sufficient sample length to give a stable spectral estimate and short enough to exclude most of the signal coda. The effect of the signal length on the shape of the estimated power spectra is tied to the degree of nonstationarity of the P wavetrain. In order to reduce the variability, the spectra were smoothed by averaging the frequency components over a 1.0 Hz bandwidth. For our purpose, the loss of frequency resolution by this procedure was insignificant.

SIGNAL LOSS IN BEAMFORMING

The characteristic feature of an array is, as mentioned previously, its ability of suppressing noise. The gains in SNR using the simple but effective sum-and-delay processing or beamforming is proportional to (no. of sensors)$^{\frac{1}{2}}$ under the assumption that the noise is a random Gaussian process and signals identical across the array. The latter hypothesis is not quite correct for short period P-waves due to small signal dissimilarities and inevitable errors in measuring beamsteering delays (Bungum & Husebye, 1970). The time delays between subarrays were computed using an iterative cross-correlation procedure to ensure proper signal line-up. Within subarrays, delays between the sensors were calculated from the apparent direction of approach and velocity of the wave front observed by the array. All the individual traces from single sensors were plotted prior to analysis. Because of the generally good S/N ratio, we could visually observe that major peaks or throughs in the delayed signals were in phase within one sample or 0.05 seconds for many subarrays, whereas in some cases time anomalies up to 0.2 seconds were observed (see Fig 1).

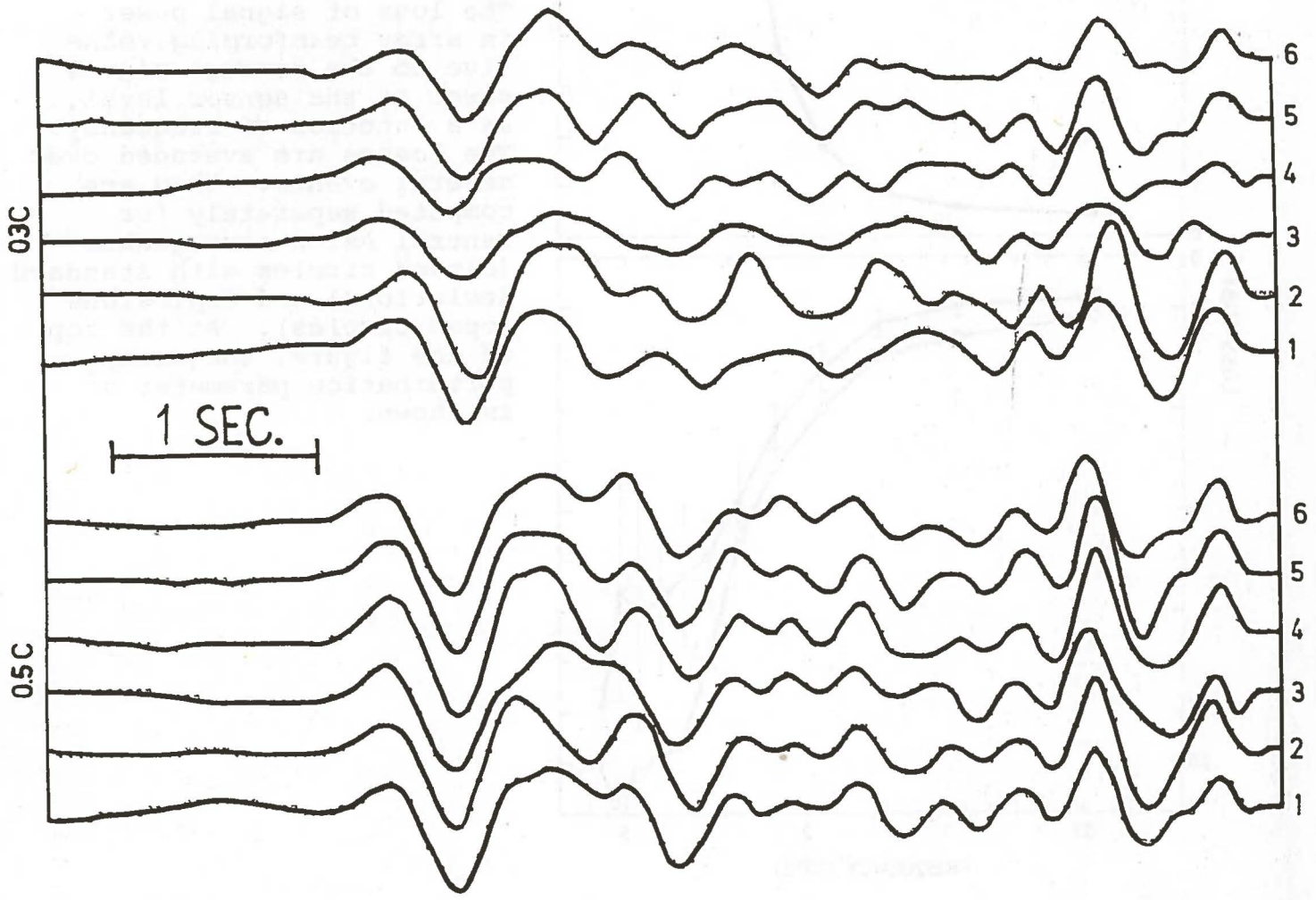

Fig 2. P wave signals recorded from the earthquake of 02 Jan 1972 in Sinkiang, China, at two of NORSAR's subarrays. At subarray 05C the signals are in phase, at 03C apparently not.

The signal power loss on both the array and subarray level has been computed according to equation (8) and in the latter case is defined as the ratio between subarray beam power and the average of the single sensor power within the subarray. The results obtained, including the array and subarray perturbation parameters σ^2 and σ^2_s are displayed in Figs 3 and 4.

A few comments to the presented results are as follows: The dominant trend in both figures is the rapid increase in beam power losses for frequencies larger than 1 Hz. The gradient of the loss curves is around 4 and 10 dB/octave for the subarray and array beams respectively. This means that spectraform processing schemes of array

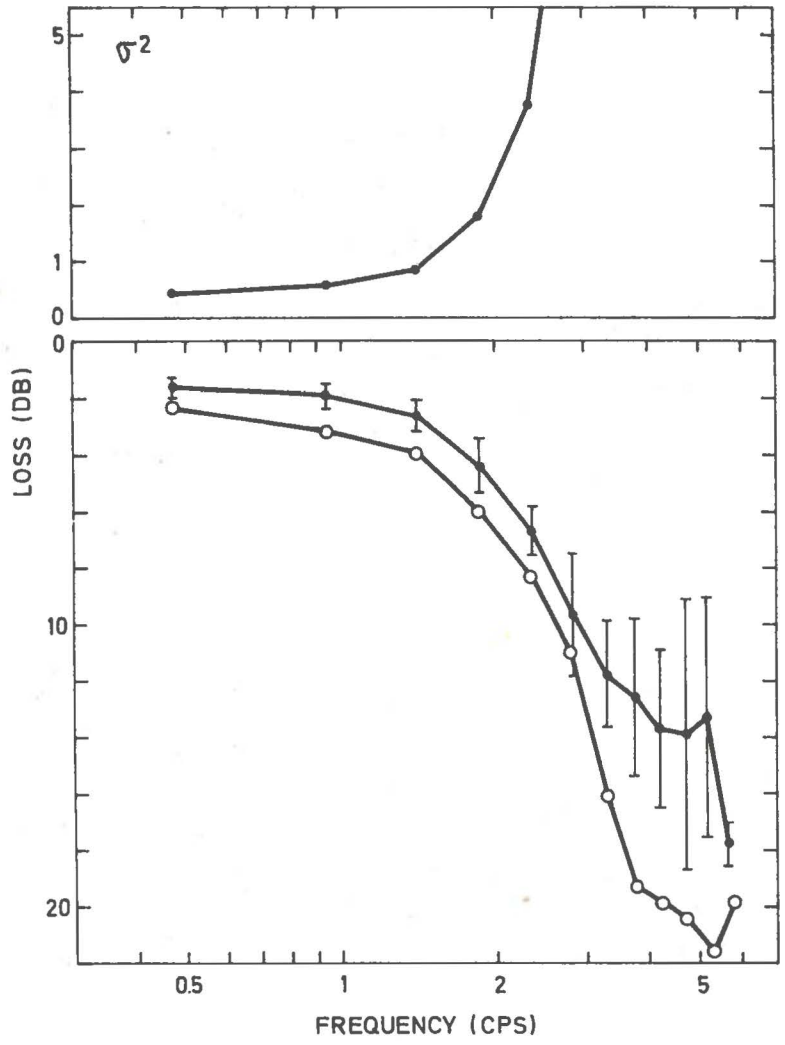

Fig 3.

The loss of signal power in array beamforming relative to the average signal power at the sensor level, as a function of frequency. The losses are averaged over several events. They are computed separately for Central Asian earthquakes (closed circles with standard deviations) and explosions (open circles). At the top of the figure, the array perturbation parameter σ^2 is shown.

data, either in time or frequency domain, would always give a relative SNR maximum at a frequency which is higher than the corresponding value for ordinary beamforming processing. Moreover, at a frequency around 3 Hz the signal suppression due to beamforming amounts to around 50% of the noise suppression. We, and others like Harley (1972) also find that the noise reduction, as expected, is proportional to (no. of sensors)$^{\frac{1}{2}}$ and uniform for all frequencies.

A comparison between our observations, based on a few NORSAR recorded P-signals, and corresponding results of Lacoss & Kuster (1970), based on a few LASA-recorded P-signals, exhibit a remarkably good agreement concerning the beam loss and signal perturbation parameters. This is somewhat contrary to expectations as signal coherency is better across LASA than NORSAR (Dean 1966, Bungum et al 1971). A likely explanation is the difference in signal sample length, as 6.4 and 10.0 sec were used respectively.

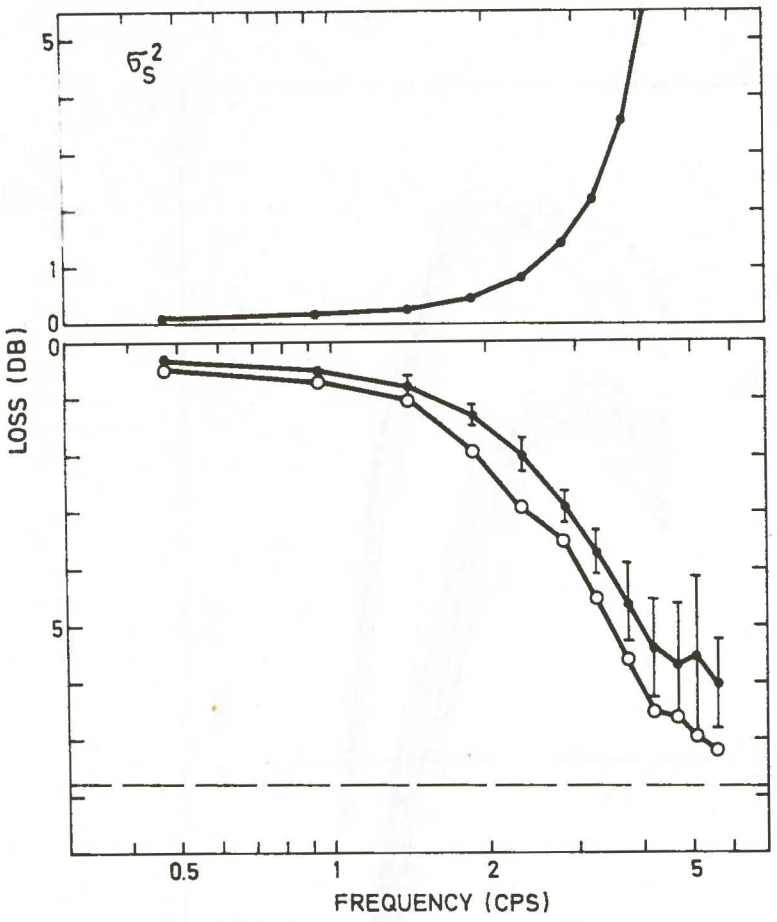

Fig 4.

The loss of signal power in subarray beamforming relative to the average signal power at the single sensor level, as a function of frequency. The losses are averaged over all subarrays and several events. They are computed separately for Central Asian earthquakes (closed circles with standard deviations) and explosions (open circles). At the top of figure, the subarray perturbation parameter σ_s^2 is shown.

It should be remarked that the result presented in this section, besides being based on few events, represents idealized array operational conditions, i.e., using the very best beamsteering delays available. In practice, and especially for weak events where precise epicenter location information is not available, the gradient of the high-frequency beam losses would probably be closer to 20 dB/octave than 10 dB/octave.

SHAPE OF SIGNAL SPECTRA

The power spectra of the 9 shallow earthquakes and 6 underground explosions in Central Asia listed in Table 1 are shown in Fig 5. All spectra are normalized to equal total power. The quakes occurred within a limited region and were in the magnitude range 5.2 to 6.0. The explosions occurred in Eastern Kazakh and were in the magnitude range 5.2 to 5.8. We computed averages of spectra separately for the two groups of events. The averages are shown in Fig 6 together with the spectrum of the explosion in western North America. Distances from NORSAR to the earthquakes are between 40 and 50 degrees,

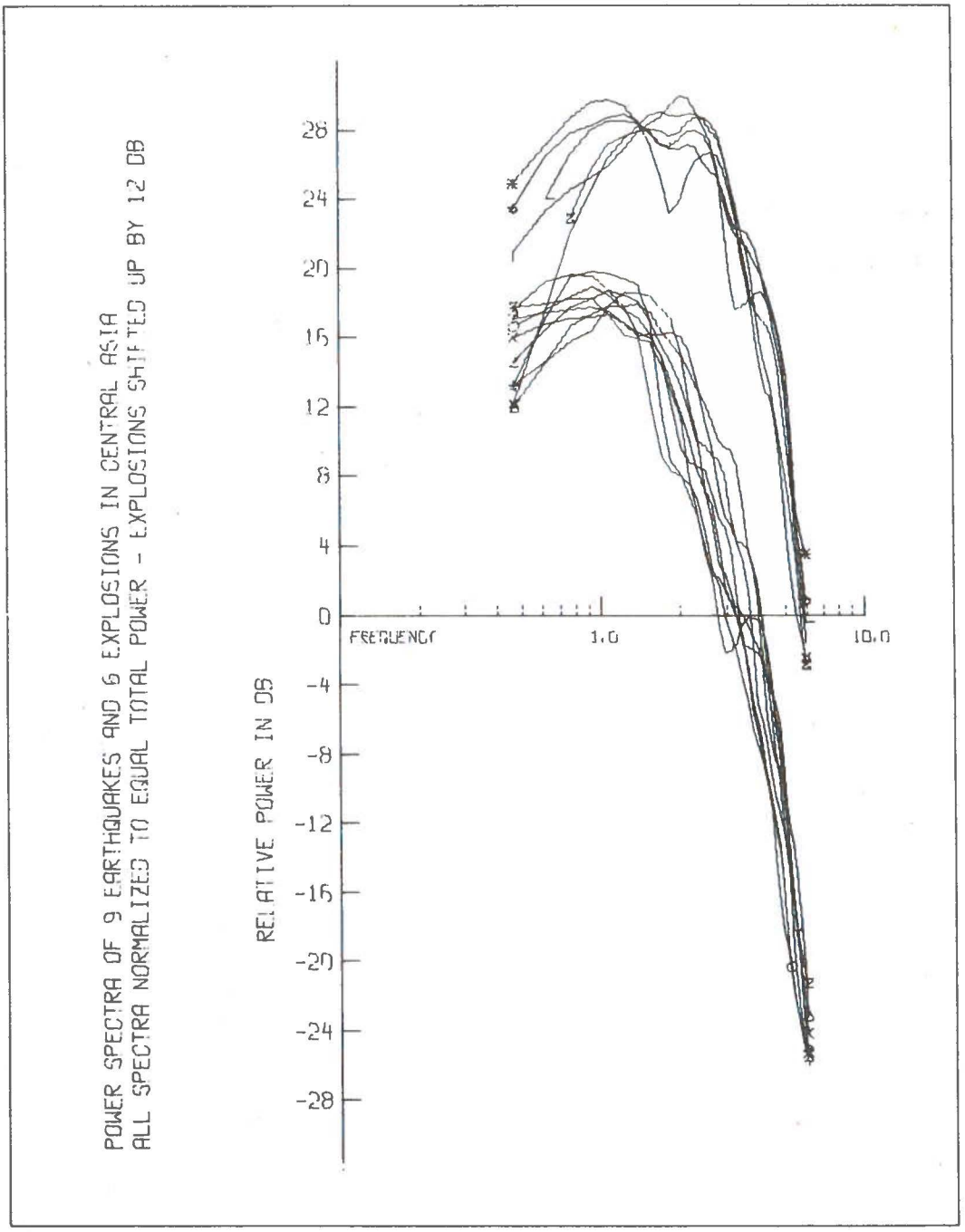

Fig 5. Observed signal spectra from a group of earthquakes and from several underground explosions, all in Central Asia. Spectra are normalized and smoothed, explosion spectra are shifted upwards in figure for clarity. The cuts in explosion spectra produced by the interference of surface-reflected waves are visible, but the frequencies seem to vary in the event population considered.

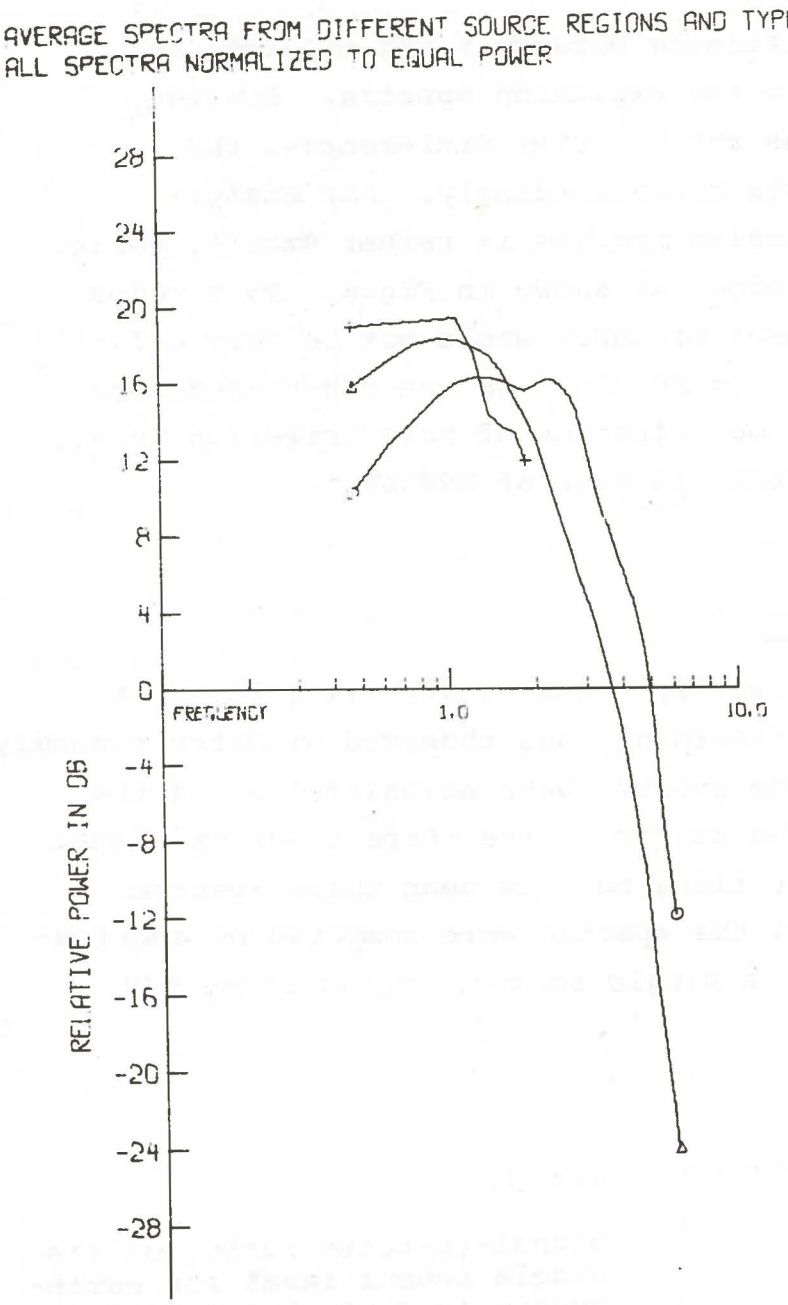

Fig 6. Averages of spectra from earthquakes and explosions in Central Asia, curves marked with circles and triangles at the ends, respectively. The spectrum of an explosion in North America is marked with crosses. The average Central Asian explosion spectrum has a shift of energy towards high frequencies relative to spectrum of earthquakes at the same region and relative to the explosion in North America.

to the explosions in Asia 38 degrees and to the explosion in North America 74 degrees. The explosions in Asia have a spectrum different from the earthquake group having more energy at high frequencies, as has been observed earlier, (e.g., Lacoss 1969, Weichert 1971). Hasegawa (1972) has shown that the difference in shape is due both to the weaker generation of long wavelengths by the explosion or point source and the shallow depth of explosion producing significant destructive interference between P and pP waves.

The explosion in North America has no energy enrichment towards higher frequencies as compared to those in Central Asia. This difference **in** the spectra of explosions being in the same magnitude range can be accounted for by taking the attenuation parameter t* to be larger by 0.5 for the ray path from the explosion site in North America to NORSAR relative to the ray paths from Central Asia, if the total nonelastic attenuation of waves is of the form $\exp(-\pi f t^*)$ where f is frequency. We should here like to add that in case of NORSAR earthquake recordings, the signal high-frequency content is primarily governed by the seismic regions and not azimuth and epicentral distance.

The mentioned destructive interference between P and pP waves is most often observable as cuts in the explosion spectra. However, due to variations in shot depths and velocity differences, the spectral irregularities fluctuate correspondingly. For example, the sum of 6 Central Asian explosion spectra is rather smooth, while the individual variations are large, as shown in Fig 6. This means that a spectral ratio discriminant probably would not be very efficient in general and not at all for NORSAR. On the other hand, the 3rd moment discriminant or some modification of this criterion (e.g., Anglin 1972) is likely to be useful in case of NORSAR.

SIGNAL-TO-NOISE RATIOS AT NORSAR

We have computed a mean noise power spectrum by averaging 15 noise power spectra obtained by spectraforming, and observed at dates randomly distributed within one year. The spectra were normalized so as the total power to become unity. The ratios of the three types of signal spectra described in previous sections to this mean noise spectrum are shown in Fig 7. Because all the spectra were computed by spectraforming, the S/N ratios are for a single sensor. To estimate S/N

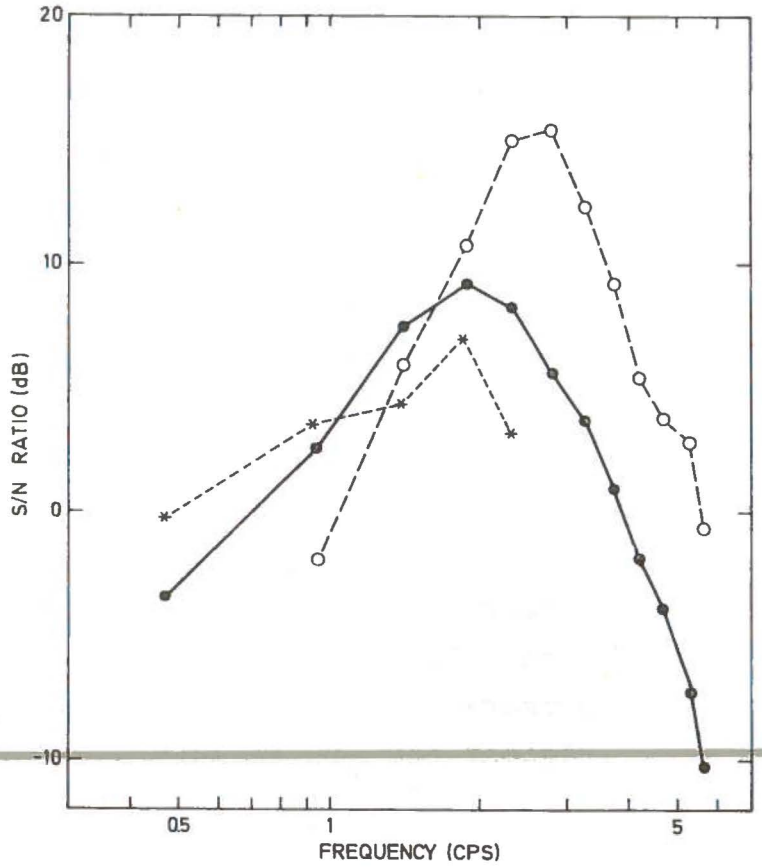

Fig 7.

Signal-to-noise ratios on the single sensor level for earthquakes in Central Asia (closed circles), underground explosions in Central Asia (open circles) and for an explosion in western North America (asterisks). Both the noise and signal are averages over ensembles of data, and they have normalized to unit total power prior to taking ratios. The absolute levels of the displayed ratios would be achieved for events with m_b around 4.7-4.8 in Central Asia and somewhat larger than 5.0 for explosions in North America.

ratios for subarray and array beams, the suppression of noise and the beam loss of signal as given in Figs 3 and 4 have to be taken into account. The absolute levels of the displayed S/N ratios are determined by the fact that each spectra used in computing them was normalized to have unity power at the output of the short period recording system.

The flat character of the S/N ratio of the event in North America is contrasting to events in Central Asia which peak at significantly higher frequencies. In general, the noise spectrum varies slowly in time, but the P-signal spectrum is mainly dependent on the individual seismic active regions. This simply means that the SNR as a function of frequency varies randomly within a certain frequency interval, and thus a large degree of flexibility is required in certain array processing schemes to ensure at least approximately optimum performance. For example, the NORSAR event detection processor has only one bandpass filter available for additional noise suppression due to hardware limitations, and the 1.2-3.2 Hz filter in use has been selected on the basis of a best-in-average criterion.

An interesting aspect of the general problem outlined above is whether spectraform processing in frequency or time domain represents a viable alternative to conventional beamforming or sum-and-delay processing. A comparison of the relative advantages of the two fundamentally different array processing procedures can be achieved by computation of stabilities, which are defined as the ratio of the square of expected noise-corrected signal power to the expected variance of the same quantity.

Again following Lacoss and Kuster (1971) we may express spectraform stability s_p and beamform stability s_b as given below:

$$s_p = \frac{Kr^2}{2r+1+K/L} \tag{9}$$

$$s_b = \frac{Kr^2}{g^2\left(\frac{2r}{g}+\frac{1}{K}\left(1+\frac{1}{2}\right)\right)} \tag{10}$$

where K is the number of sensors, L is the number of blocks used in estimation of noise, r is the expected SNR on the single sensor level and $g^{-1}=B/P$ is the beam loss. As a specific example, the beam loss

and SNR as a function of frequency, determined for an average earthquake of the group in Central Asia and scaled down to magnitude 4.8, are put into equations (9) and (10). The computed stabilities are shown in Fig 8. In addition to the requirement of stability, the observation of signal spectrum is limited by the fact that the signal plus noise-to-noise ratio must be sufficient to make sure that signal is really present at a certain frequency. For our observational conditions this requirement is fulfilled at signal-to-noise ratios of 0 dB and 5.5 dB on a single sensor and the beam, respectively.

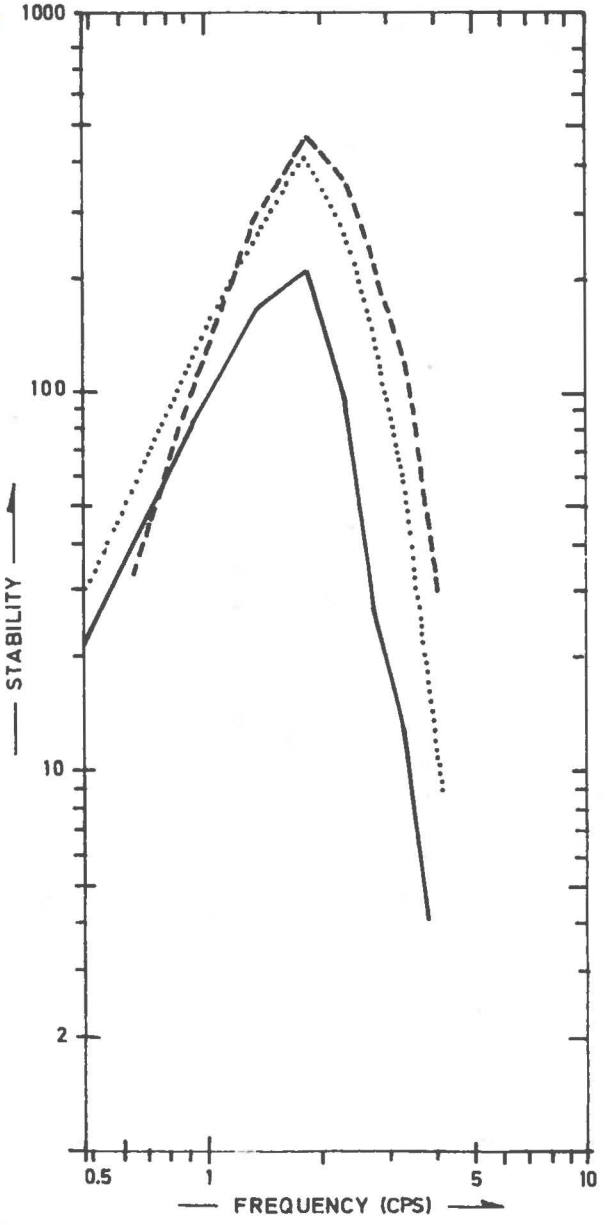

Fig 8. Stabilities for different forms of processing array data, computed from loss and SNR observations for the earthquakes in Central Asia, scaled to m_b 4.8. Continuous line is beamforming, broken line is spectraforming and dotted line is spectraforming of subarray beams.

The stability of the spectrum computed by spectraforming is larger at frequencies above about 1 cps. Both forms of processing stop at about 4 cps because of the requirement of 99% confidence on signal presence. However, at that frequency the stability of averaged (spectraform) spectrum is around 30 while the corresponding beam spectrum stability is 2.

It is obvious that the benefits of spectraforming in case of a relatively incoherent and/or high-frequency signal would be even more evident at the high frequencies. For that type of P-signal spectraforming would be a better data processing procedure above a certain signal frequency. Such signals are often recorded at the NORSAR array for epicentral distances less than, say, 35 degrees.

As a combination of spectraforming and beamforming, one could also compute the average spectrum of subarray beams. That appears to have a good stability at a wide range of frequencies, and relevant results are also plotted in Fig 8. The main advantages of the above combination is that subarray beamforming gives a sixfold suppression in noise power in case of NORSAR while the signal subarray beam loss is modest, even for poor epicenter locations. Moreover, the spectraform operation gives a reduction of noise variance of $\sqrt{22}$ = 6.80 dB.

DISCUSSION

From the results presented in the previous sections, it is obvious that for certain seismic events spectraform processing gives more stable spectral estimates than array beam processing does. This point is very important when designing spectral classification criteria like spectral ratio (Kelly 1968) and 3rd moment using short period P-signals (Anglin 1972). These discriminants take advantage of the relatively large high-frequency energy in explosion generated P-waves which may be partly lost during processing as demonstrated in this paper. The same argument applies to time domain complexity classification criteria, as strong signal coda suppression occurs during beamforming. Thus, in order to ensure optimum performance of these short period P-wave discriminants, both spectraform and beamform processing techniques should be applied.

From a computational point of view, beamforming or the combined beamform/spectraform discussed in the previous section is most attractive as time domain array and subarray beams are created automatically for all NORSAR recorded events. Spectraforming itself, i.e., in case of NORSAR requiring 132 single sensor spectra, is very time consuming (around 50 min of computer time), but its relative advantage to the combined spectraform-beamform is modest (see Fig 8). The latter statement has also been confirmed by Dahle (personal communication) as he finds high signal similarities within NORSAR subarrays. Another argument here is that in general beamforming stability as compared to that of spectraforming increases with decreasing signal power.

Finally, we should like to remark that time domain processing schemes equivalent to frequency domain spectraforming would naturally give more stable SNR estimates for relatively incoherent and/or high-frequency signals as compared to conventional beamforming. An example here is

that the NORSAR detection processor system (see Bungum et al, 1971) has been supplemented with a detector where the array beam is taken as the rectified average of high-frequency bandpass filtered subarray beams. According to Ringdal (personal communication) the "beamform/ spectraform" processor has a better event detection performance than the corresponding array beamforming detector for epicentral distances less than around 35 deg.

ACKNOWLEDGEMENTS

This study was undertaken during the stay of one of the authors, I. Noponen, at NORSAR, Norway. He was supported from a grant for Nordic cooperation in seismology, given to the Institute of Seismology, University of Helsinki by the Ministry of Education, Finland.

This research was supported by the Advanced Research Projects Agency of the Department of Defense and was monitored by the Air Force Office of Scientific Research under Grant No. AFOSR-72-2377.

The NORSAR research project has been sponsored by the United States of America under the overall direction of the Advanced Research Projects Agency and the technical management of Electronic Systems Division, Air Force Systems Command, through Contract No. F19628-70-C-0283 with the Royal Norwegian Council for Scientific and Industrial Research.

REFERENCES

1. F.M. Anglin: Short period discrimination studies using the Yellowknife seismological array data, Proceedings, Seminar on Seismology and Seismic Arrays, Oslo, Nov 1971, 1972.

2. H. Bungum and E.S. Husebye: Errors in time delay measurements, Pure and Appl. Geophys., 91, 56-70, 1971.

3. H. Bungum, E.S. Husebye and F. Ringdal: The NORSAR array and preliminary results of data analysis, Geophys. J.R. Astr. Soc., 25, 115-126, 1971.

4. W.C. Dean: Preliminary plans: SDL processing of LASA data, First LASA Systems Evaluation Conference, 14-16 September 1965.

5. T.W. Harley: Preliminary evaluation of the NORSAR short period and long period arrays, Proceedings, Seminar on seismology and seismic arrays, Oslo, 22-25 Nov 1971, 1972.

6. H.S. Hasegawa: Analysis of amplitude spectra of P waves from earthquakes and underground explosions, J. Geophys. Res., 77, 3081-3096, 1972.

7. E.J. Kelly: A study of two short-period discriminants, Tech. Note 1968-8, Lincoln Lab MIT, 1968.

8. R.T. Lacoss: LASA Decision probabilities for M_s-m_b and modified spectral ratio, Tech. Note 1969-40, Lincoln Lab MIT, 1969.

9. R.T. Lacoss and G.T. Kuster: Processing a partially coherent large seismic array for discrimination, Tech. Note 1970-30, Lincoln Lab MIT, 1970.

10. D.H. Weichert: Short period spectral discriminant for earthquake-explosion differentiation, Zeitschrift für Geophysik, 37, 147-152, 1971.